Acta Oceanol. Sin., 2018, Vol. 37, No. 5, P. 13–21
DOI: 10.1007/s13131-018-1210-8
http://www.hyxb.org.cn
E-mail: hyxbe@263.net

The relationships among aerosol optical depth, ice, phytoplankton and dimethylsulfide and the implication for future climate in the Greenland Sea

QU Bo[1]*, GABRIC Albert J.[2], ZHAO Li[1], SUN Wenjing[3], LI Hehe[4], GU Peijuan[5], JIANG Limei[6], ZENG Meifang[7]

[1] School of Science, Nantong University, Nantong 226019, China
[2] School of Environment, Griffith University, Nathan, Qld 4111, Australia
[3] Jurong Country Garden School, Zhenjiang 212400, China
[4] Chinese Sinosoft Company Limited, Beijing 100190, China
[5] Nanjing Kangni New Energy Auto Part Co., Ltd, Nanjing 210000, China
[6] College of Basic Education, Nantong Institute of Technology, Nantong 226002, China
[7] Primary School Department, Kunshan International School, Kunshan 215300, China

Received 19 September 2017; accepted 28 December 2018

Abstract

The sea-to-air flux of dimethylsulphide (DMS) is one of the major sources of marine biogenic aerosol, and can have an important radiative impact on climate, especially in the Arctic Ocean. Satellite-derived aerosol optical depth (AOD) is used as a proxy for aerosol burden which is dominated by biogenic aerosol during summer and autumn. The spring sea ice melt period is a strong source of aerosol precursors in the Arctic. However, high aerosol levels in early spring are likely related to advection of continental pollution from the south (Arctic haze). Higher AOD was generally registered in the southern part of the study region. Sea ice concentration (SIC) and AOD were positively correlated, while cloud cover (CLD) and AOD were negative correlation. The seasonal peaks of SIC and CLD were both one month ahead of the peak in AOD. There is a strong positive correlation between AOD and SIC. Melting ice is positively correlated with chlorophyll *a* (CHL) almost through March to September, but negatively correlated with AOD in spring and early summer. Elevated spring and early summer AOD most likely were influenced by combination of melting ice and higher spring wind in the region. The peak of DMS flux occurred in spring due to the elevated spring wind and more melting ice. DMS concentration and AOD were positively correlated with melting ice from March to May. Elevated AOD in early autumn was likely related to the emission of biogenic aerosols associated with phytoplankton synthesis of DMS. The DMS flux would increase more than triple by 2100 in the Greenland Sea. The significant increase of biogenic aerosols could offset the warming in the Greenland Sea.

Key words: dimethylsulfide flux, sea ice, chlorophyll, aerosol optical depth, Greenland Sea

Citation: Qu Bo, Gabric Albert J., Zhao Li, Sun Wenjing, Li Hehe, Gu Peijuan, Jiang Limei, Zeng Meifang. 2018. The relationships among aerosol optical depth, ice, phytoplankton and dimethylsulfide and the implication for future climate in the Greenland Sea. Acta Oceanologica Sinica, 37(5): 13–21, doi: 10.1007/s13131-018-1210-8

1 Introduction

Atmospheric aerosols are derived from anthropogenic and natural sources. During the Arctic spring, the local aerosol burden maybe influenced by anthropogenic, marine and continental sources (Barrie, 1995). The "Arctic haze" is due to northerly transport of pollution from anthropogenic activities, and has a warming effect on the regional climate (Zhao and Garrett, 2014). Conversely, the emission of biogenic sulfate aerosols during the biologically productive season may offset climate warming. Biogenic sulfate aerosols are produced by oxidation reactions in the atmosphere from gaseous precursors such as dimethylsulfide (DMS) emitted by the marine food web (Charlson et al., 1987). It has been suggested that the greatest perturbation to DMS flux under warming will occur at high latitudes in both hemispheres, with little change simulated in the tropics and sub-tropics (Gabric et al., 2004, 2013).

In remote marine atmospheres, aerosols consist of sea salt particles, organics and sulphate from the oxidation of biogenic DMS (Andreae, 2007). Sea salt is a major component of marine aerosol when wind speeds are high (Meskhidze and Nenes, 2010). Sea ice loss in the Arctic is an indirect source of sea salt aerosols, as the rapid decrease of sea ice cover in recent decades which leads to an increase in the area of open water, resulting in sea salt aerosol emissions increasing, in turn leading to an increase in satellite-derived aerosol optical depth (AOD) in 70°–80°N (Struthers et al., 2011). Osto et al. (2017) (www.nature.com/scientificreports) found that the majority of the ultrafine aerosols were associated with air masses travelling over open water (43%–51%) and sea ice (29%–39%). The area with melt ponds, open leads amidst the pack ice and ice floe, are all the strong

Foundation item: The National Natural Science Foundation of China under contract No. 41276097.
*Corresponding author, E-mail: qubo@ntu.edu.cn

sources of precursor gas of aerosols in summer Arctic. Ice melting is also a significant source of ammonium. Decrease of ice alters marine ecosystems by increasing the rates of phytoplankton by 20%–30%.

The non-sea salt aerosol includes sulfate, particulate organic matter, mineral dust and black carbon. DMS is the main biogenic sulfate aerosol released from the Arctic Ocean (Ferek et al., 1995). As sea ice recedes in the Arctic, phytoplankton growth occurs in open waters, and trapped DMS is released from the ice matrix as well as from blooms in the newly formed open leads. As a consequence, the peak in DMS would occur after the phytoplankton bloom (Gabric et al., 2005).

Aerosol-cloud-climate interactions are closely connected. Curry (1995) has suggested that rising temperatures would lead to a reduction in sea ice and snow extent, hence reduce the polar surface albedo, cause further climate warming. Charlson et al. (1987) suggested there are direct and indirect radiative effects of biogenic aerosols in the troposphere, with both effects possibly offsetting the effects of warming (Leck and Persson, 1996).

Cloud cover in the Arctic has different climate impacts in winter and summer. Cloud reduces surface heating during summer time, and reduces surface cooling during winter time (Curry et al., 1996). About 40% of Arctic cloud cover is made up of thin single-layer clouds with bases below 2 km (Zhao and Garrett, 2014). Arctic haze influences aerosol composition especially during winter and early spring when continental forest fires have a seasonal maxima (Quinn et al., 2007). The changes of winter cloud would alter the AOD signal. There is a negative correlation between winter time cloud fraction and AOD in the Arctic (Struthers et al., 2011). The natural aerosol includes sea salt and biogenic marine sources. In the Arctic Ocean, black carbon and mineral dust aerosols are a smaller component of total AOD. The radiative balance in the Arctic may be largely affected by the changes in surface albedo (decrease) and sea salt aerosol (increase) due to the loss of Arctic sea ice (Struthers et al., 2011). Cloudiness and cloud radiative forcing are strongly coupled to Arctic sea ice cover (Struthers et al., 2011). Clouds are major source of uncertainty in climate model predictions. Cloud cover and albedo may have strong impact on the summer ice melting. Increased cloud cover in Arctic could lead to warming and accelerated sea-ice melting (Osto et al., 2017). Increasing in sea salt particles can affect CDNC (cloud droplet number concentration), but this must be accompany by an increased surface wind speed over the bloom (Meskhidze and Nenes, 2010). Hu et al. (2011) studied the AOD around China's seas during 1980–2001 and found the increase of AOD would result in the decrease of the maximum temperature rather than minimum, with decrease of 0.11/0.08 K for zonal average.

Due to less pollution, remote polar regions are ideal places for examining the effects of marine productivity and biogenic aerosol emissions on clouds. In this work, we examine the relationship between DMS and DMS flux with sea ice concentration (SIC), the relationship among AOD with SIC, cloud cover (CLD), and surface chlorophyll *a* (CHL) in the Greenland Sea (65°–80°N), a region of importance for both the polar and global climate, and describe the key factors influencing the seasonal cycle of these parameters. Furthermore, the DMS flux would be predicted for year 2100 under 4×CO_2 scenario. The implications of future climate in the Greenland Sea would be investigated.

2 Data sources and methods

We focus on the Greenland Sea (65°–80°N, 20°W–10°E) (Fig. 1) for the period 2003–2012. The highlighted study region in Fig. 1 also includes part of the Iceland Sea and Norwegian Sea. Global data on CHL and aerosol optical depth are obtained from the MODIS (Aqua) satellite 8-day, level 3 archive, at a resolution of 4-km (http://oceandata.sci.gsfc.nasa.gov/MODIS-Aqua/Mapped/8Day/4km). SIC is obtained from the NOAA archive at iridl.ldeo.columbia.edu/SOURCES/.NOAA (Reynolds et al., 2002) with resolution of 1°×1°. Surface wind speed and direction are obtained from Remote Sensing Systems (REMSS: www.remss.com/windsat). CLD is calculated from the NASA archive available at http://gdata1.sci.gsfc.nasa.gov/daac-bin/G3/. The SeaDAS 6.4 image analysis package data analysis system is used to subset and analyze the regional AOD and CHL data (seadas.gsfc.nasa.gov/). Mixed layer depth (MLD) is calculated using

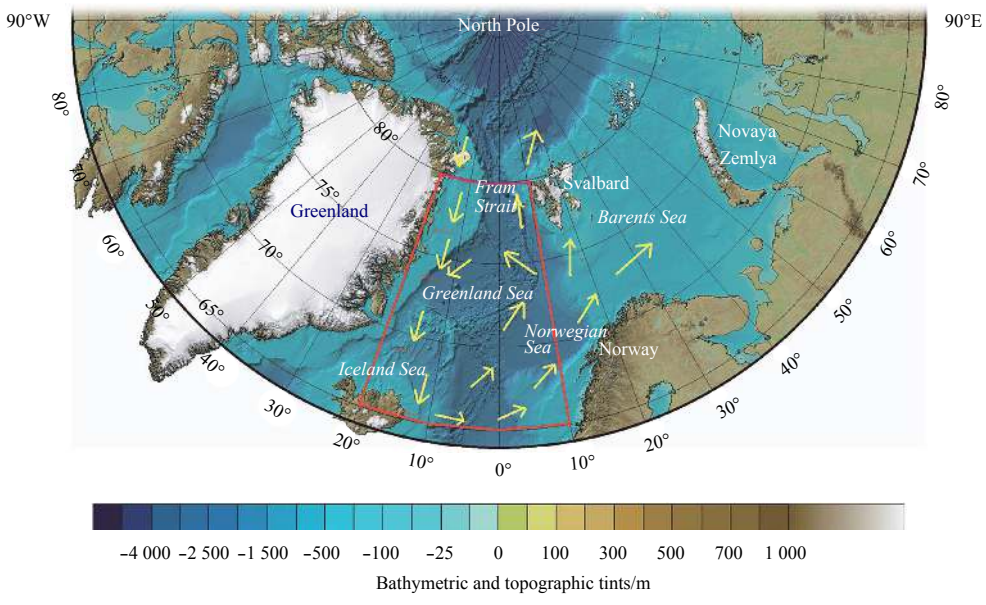

Fig. 1. Map of study region with topography. Red box denotes the study region (65°–80°N, 20°W–10°E) mainly in the Greenland Sea and yellow arrows the surface current directions.

CTD (conductivity, temperature, depth) data available from the Arctic Ocean Measurement Database (http://oregon.iarc.uaf.edu/dbaccess.html). MLD is computed based on constant temperature difference criterion (0.5°C between the surface and bottom). Missing values are replaced by using the five nearest values. Spatial-temporal gridding of MLD of 1°×1° is calculated using *R* statistical software (Qu et al., 2016b). Missing monthly data is inserted by using interpolation of adjacent month data.

The Coupled Model Intercomparison Project Phase 5 archive (CMIP5) (http://pcmdi9.llnl.gov/cmip5/forcing.html) is used to provide forcings under the warming scenarios. Software OpenLDAP (an open source implementation of the Lightweight Directory Access Protocol) is used to retrieve the forcing data in AMIP for SST, CLD, SIC, WIND (wind speed) and MLD for 4×CO_2 conditions.

Correlations and lagged regression analysis for AOD, SIC, CLD and CHL were computed using the statistical software package Eviews and SPSS.

The accuracy of satellite data (especially for the remote Arctic Ocean) would relate directly to the reliability and accuracy of this study. Surface chlorophyll concentration, aerosol optical depth and photosynthetically active radiation (PAR) were obtained from the level-3 MODIS (Aqua) (http://oceandata.sci.gsfc.nasa.gov/MODIS-Aqua/Mapped/8Day/4km) (Moderate Resolution Imaging Spectroradiometer) have unprecedented onboard calibration systems enabling monitoring of its performance and correcting for the errors introduced into the data by system degradation. NASA Goddard Space Flight Center has managed to improve the accuracy of the ocean color products (http://modis.gsfc.nasa.gov/MODIS/CAL/#intro). Spectroradiometric Calibration Assembly (SRCA) is for checking the radiometric, spectral and geometric properties of the MODIS system. Calibrations were done for regional differences between MODIS with SeaWiFS especially for the Arctic Ocean (Bailey and Werdell, 2006). At high latitudes, multiple orbits are considered for a given *in situ* record. However, errors are unavoidable for solar zenith angles more than 70° and view angles more than 45° (Bailey and Werdell, 2006). Generally, the summer time data is more accurate. It is estimated that the satellite-derived CHL underestimates the true concentration by a factor of 1.4 when compared with *in-situ* CHL data (Bailey and Werdell, 2006). The data errors in the Arctic Ocean are well within the range of errors for global data as indicated by an evaluation done for the western Arctic Ocean (Chaves et al., 2015).

The computation of the regional means is another possible source of error due to missing data mainly caused by cloud cover.

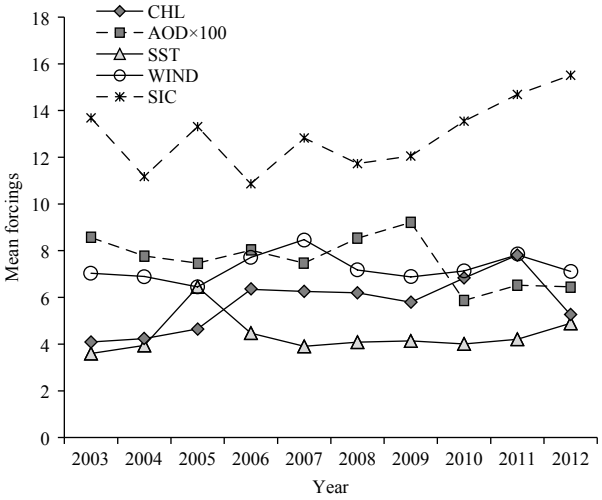

Fig. 2. Regional mean annual forcings (CHL (mg/m^3), AOD×100, SST (°C), WIND (m/s) and SIC (%)) for year 2003–2012.

The missing values occur are mostly north of 80°N. There were very few (less than 5%) missing values during May to August. The missing values were excluded for our estimates of regional means, thus calculated mean values could be slightly higher than reality.

3 Results

3.1 *Regional mean annual forcings*

Regional mean annual forcings are calculated (Fig. 2) for year 2003–2012. SIC had 27% increased rate, AOD had generally 18.8% decreased rate, but increased before year between 2007–2009, and had a big drop in year 2010. WIND had 4% increased rate, CHL had 27% increased rate and SST only 2% increased rate within these 10 years. SIC had an increased trend since year 2009. AOD had the highest peak in year 2009 and had an immediate drop in year 2010. CHL had increased trend from 2009 to 2011 and peaked in year 2011 and dropped in year 2012. Wind speed had peak year in 2007 and second peak in year 2011. SST had peak year in 2005 and decreased since year 2005, had slightly increased trend in year 2012. Generally, with the annual increased SIC, CHL also increased during the ten years,

3.2 *Regional AOD and CLD distributions*

Mean spatial distributions of AOD and CLD are shown in Fig.

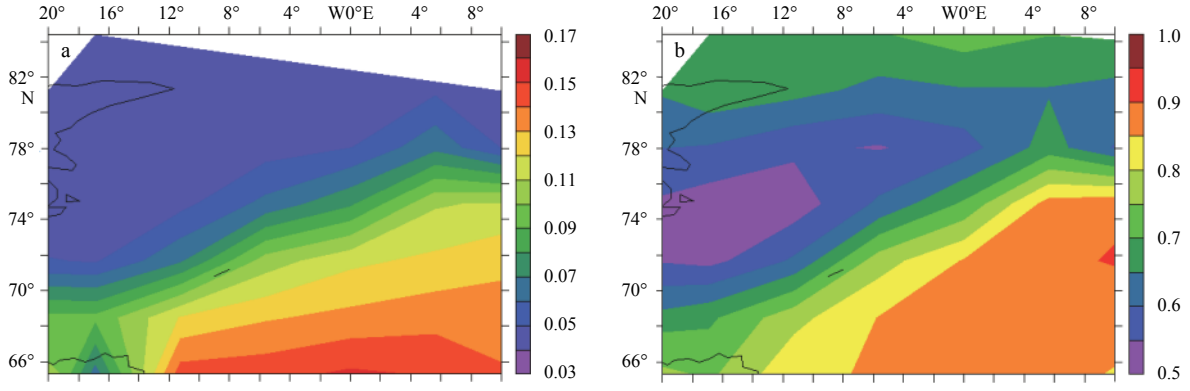

Fig. 3. Mean spatial distributions of AOD (a), and total CLD (0⩽CLD⩽1) (b) in the study region.

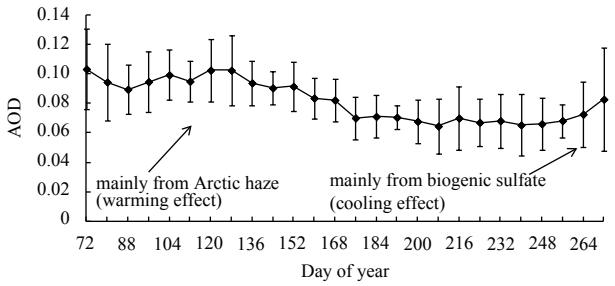

Fig. 4. Mean AOD in the study region (65°–80°N) for 2003–2012. Vertical bars are the standard deviation.

3. There is a clear meridional gradient in AOD with values higher in the south and lower in the north of the study region (Fig. 3a) and a weaker zonal gradient with higher AOD in the east, especially south of 78°N. There was higher CLD in the south (Fig. 3b).

The time series of AOD averaged over the study time period is shown in Fig. 4, with higher AOD in spring and lower in summer followed by an increase during autumn. The elevated springtime AOD is likely due to Arctic haze (Zhao and Garrett, 2014), although high wind speeds at this time could also lead to higher sea salt aerosols. Elevated autumn AOD is likely caused by biogenic aerosol emissions associated with the summer phytoplankton bloom. Arctic haze is thought to come from advection of pollution in Eurasia (Quinn et al., 2007), and is removed in summer by precipitation. The elevated spring aerosols caused by Arctic haze could lead to a warming of the climate (Spracklen et al., 2008), while emission of autumn aerosols due to the biogenic sulfate aerosols could cool the climate (Gabric et al., 2003).

The AOD for selected years is shown in Fig. 5. There is considerable interannual variability, with year 2009 having the highest summer AOD and year 2010 the lowest AOD almost throughout the year (Fig. 4). A negative correlation between AOD and CHL is reported by Qu et al. (2014) for spring and summer time. Lower AOD and higher summer CHL are observed in year 2010 (Qu et al., 2016a). High AOD during the spring of 2003 could be due to the extensive forest fires in Russia at that time (Serreze et al., 2000). Year 2008 had a longer period of higher AOD in spring and much higher AOD in September.

3.3 *Regional CHL and SIC*

Two snapshots of MODIS satellite CHL for 2010 (Day 128 in mid-April and Day 176 in late June) are shown in Figs 6a and b. Unusually high CHL was registered in the northeast of the study region in spring (red shows higher CHL values). By summer, moderate to high CHL was registered throughout the region (Fig.

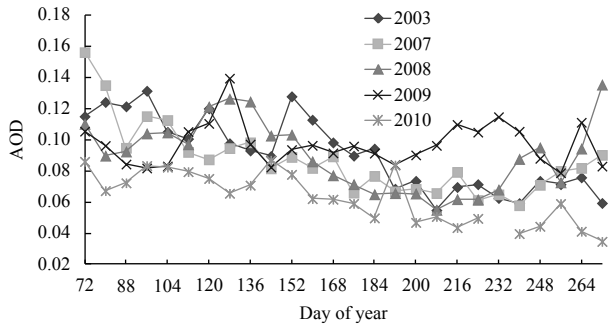

Fig. 5. Mean AOD for years 2003, 2007, 2008, 2009 and 2010 in the study region (65°–80°N, 20°W–10°E).

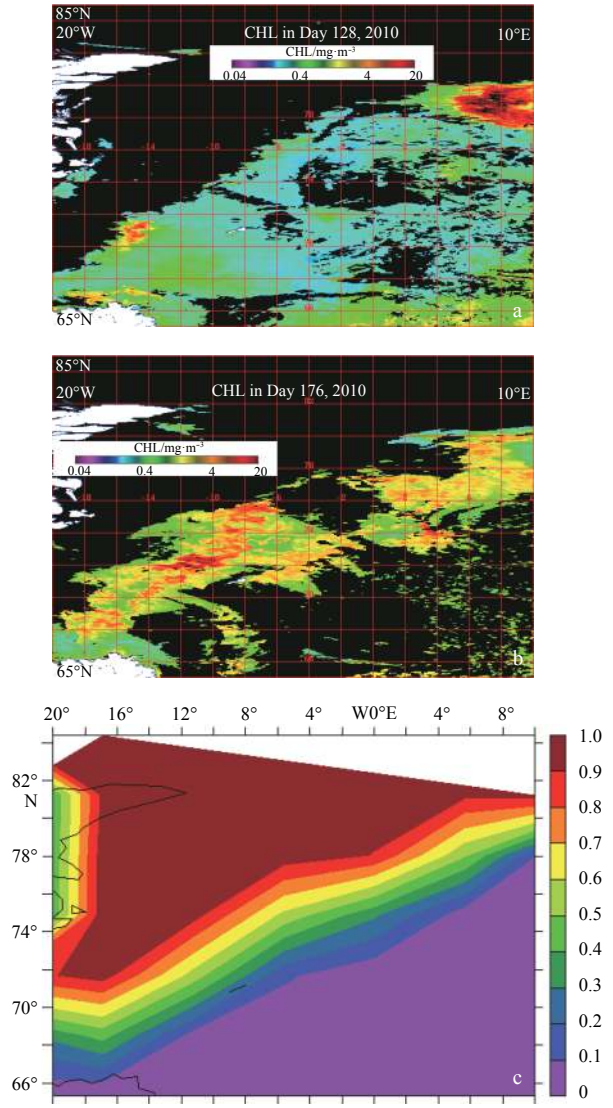

Fig. 6. CHL satellite images in Day 128 (a) and Day 176 (b) in year 2010, and annual mean SIC profile in the study region (0≤ SIC≤1) (c). Black indicates missing data due to sea ice or cloud.

6b). Mean annual SIC in the study region (Fig. 6c) displays a strong zonal gradient, likely due to the effect of the warm North Atlantic Drift in the east of the region (Fig. 1).

Figure 7a highlights the strong inter-annual variability in CHL in the sea ice covered northern part of the study region (75°–80°N). The timing of the seasonal peak in CHL varies from May to July which could be due to numerous factors, including variability in winter SIC and melt water runoff from the Greenland Glacier in eastern Greenland. Glacial melt water increases vertical stability of the water column and possibly delivers iron, a micronutrient which can favor phytoplankton growth (Levasseur, 2013). Figure 7b shows that there is a general north-south gradient in CHL with higher values in the southern part of the study region. However, elevated CHL in the north of the study region was recorded in year 2010 (Qu et al., 2016a).

Profiles of mean SIC over the selected years are shown in Figs 8a and b. The years were selected from the most variable years. Hence, the selection of years is different for south and north regions. Generally, SIC reaches a peak in March and decreases to a minimum in August to September. Both inter-annual and meri-

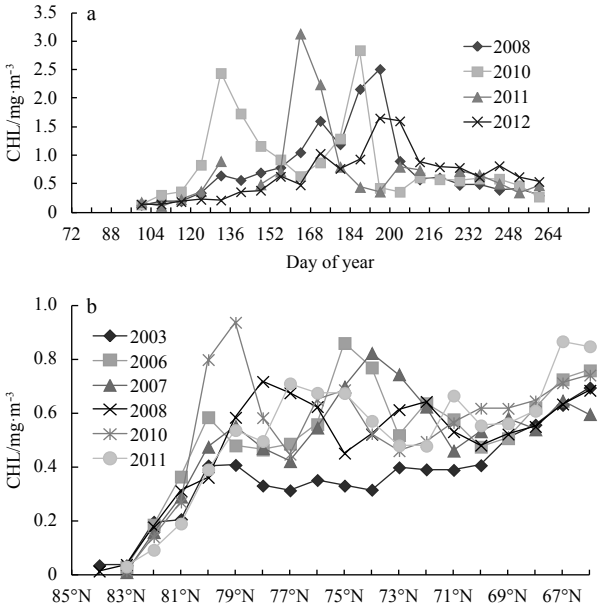

Fig. 7. Mean CHL in northern region (75°–80°N, 20°W–10°E) in years 2008, 2010, 2011 and 2012 (a); and mean CHL along latitude in years 2003, 2006, 2007, 2008, 2010 and 2011 in the study (65°–85°N, 20°W–10°E) (b).

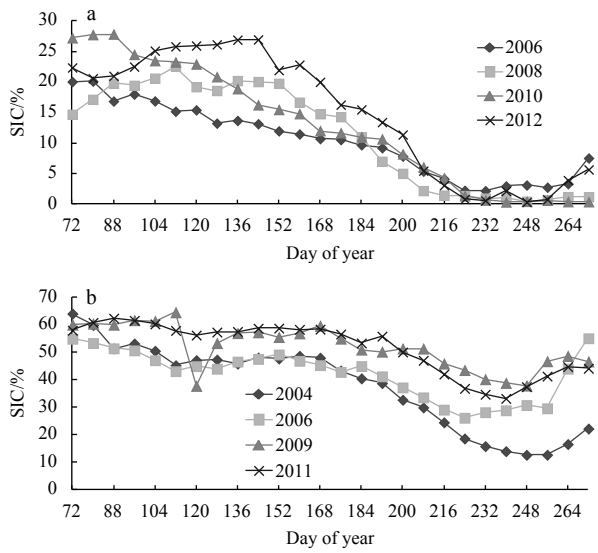

Fig. 8. Monthly mean SIC for year 2006, 2008, 2010 and 2012 in 70°–75°N (a); and monthly mean SIC for year 2004, 2006, 2009 and 2011 in 75°–80°N (b).

dional variability in SIC is evident in these figures.

3.4 *Correlation analyses*

3.4.1 *The effect of high wind speed*

We examine the possible reasons for the elevated spring and autumn AOD. Mean wind speeds and CHL are calculated for the sub-region (70°–80°N) for the ten years (2003–2012). The spring wind speed was high and above 7 m/s (Fig. 8a) with southerly direction (not shown in the figure). The high spring winds would have two effects on the aerosol: advection of pollution from continental sources (North American and East Asian sources), and

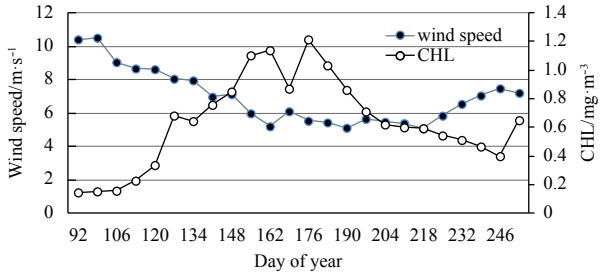

Fig. 9. Decadal mean wind speed and CHL for years 2003–2012 in 70°–80°N.

also an increase in sea salt aerosols from the ocean (Barrie, 1995). It is reported that sea salt aerosols peak mostly in the period of October to May due to stormier conditions in the Arctic Ocean and longer aerosol residence times in the Arctic. The elevated autumn wind speed (after Day 218) would have more effect on the sea salt aerosol (a cooling effect). Huang and Qiao (2009) also confirmed that the effect of wind speed over remote oceans to be significant, reporting a high linear correlation between AOD and wind speed. Figure 9 shows that wind speed is negatively correlated with phytoplankton biomass (CHL) in the spring and early summer (before Day 162). In this period, CHL increases with the decrease of wind speed. Our results show that there is inverse relationship between wind speed and CHL, with the bloom largely suppressed by high wind speed and strong vertical mixing as reported for the Southern Ocean (Fitch and Moore, 2007)

A ten-year climatology of AOD, CLD and SIC at 8-day intervals for the region 75°–80°N is shown in Fig. 10. Clear downward trends in SIC and AOD are evident during spring and summer. In general, CLD is high (around 0.8) with relatively lower CLD in April, higher CLD in summer. AOD and CLD are positively correlated in spring, but not in the autumn.

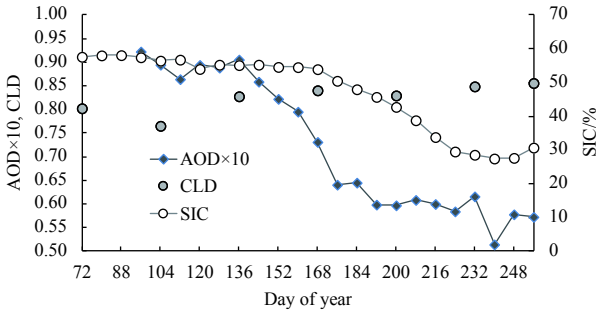

Fig. 10. Mean AOD, SIC and CLD 8-day time series in 75°–80°N for ten years.

3.4.2 *The effect of sea ice*

The rate of ice melt is calculated by computing the weekly change in SIC. Figure 11 shows the time series of ice melt, AOD and CHL for the region 75°–80°N. Ice melt started in April or May (apart from year 2007 and 2012, when melt commenced in March). The rate of ice melt dipped in May for years 2004, 2006, 2009 and 2011. In general, ice melt was positively correlated with CHL, but negatively correlated with AOD during spring and summer, and positively correlated in autumn. The region of 70°–75°N had much lower SIC and ice had little effect on CHL and AOD. The increase in AOD in late summer or autumn after the peak in CHL suggests the influence of biogenic sulfate released by phyto-

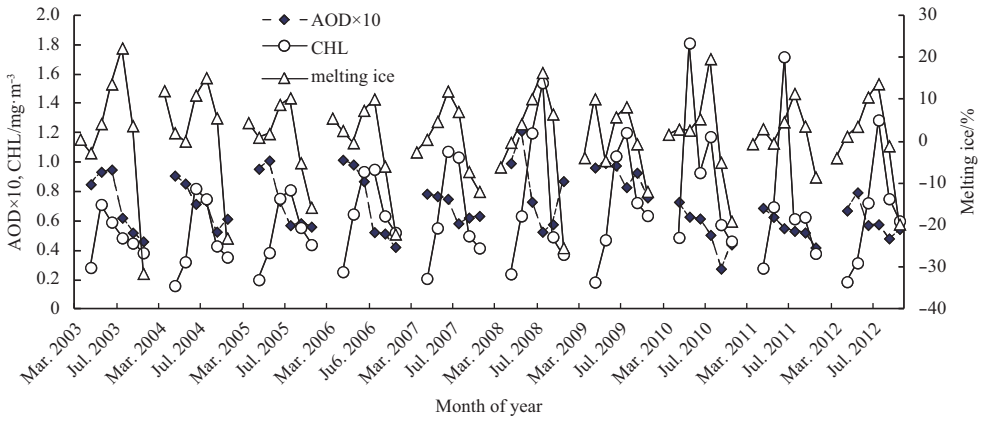

Fig. 11. Monthly mean AOD, CHL and ice melt time series in 75°–80°N.

plankton, although increased autumn wind speed, would also increase sea salt aerosols from the largely open waters.

CHL displayed an increasing trend from year 2003–2010, slightly decreasing after year 2010. The highest rate of ice melt was recorded in year 2003, with year 2010 having the second highest rate of ice melt. A second CHL bloom occurred in year 2010 at the same time as ice melt reached its maximum; AOD increased during spring and early summer in some years (2003, 2005, 2008, 2009, 2012), and then started to drop after May. Elevated AOD was influenced by combination of melting ice and higher spring wind in the region. Summer AOD decreased from June to August due to reduced wind and less ice melting together with increased sea surface temperature. After CHL bloom reached to its peak, AOD would start to increase in early autumn.

3.5 *The multivariable correlations with AOD*

When lagged, the time series of AOD and SIC display a strong correlation. However, AOD and CLD had a weaker correlation. In northern part of study region, spring AOD and SIC all had increased trends (from March to April), decreased thereafter. In the southern region, AOD reached a peak almost one month later (by May) than the southern region. AOD and SIC were negatively correlated in spring and positively correlated after spring (both decreased from May). CHL and SIC had strong negative correlations, with a reduction in SIC leading to an increase in CHL, with ice edge blooms likely contributing to the overall biomass (Levasseur, 2013).

A lagged correlation analysis was done by using the EViews software package (Pang, 2006), as shown in Table 1.

The correlation coefficients for AOD, SIC, CLD and CHL for each year are shown in Table 2. AOD and SIC, are positively correlated in most years apart from year 2009 (also see Fig. 10).

In general, the correlation between AOD and CLD, AOD and CHL were all negative, with decreased AOD accompanied by increased CLD and CHL. CHL had much improved correlations with AOD and SIC after lagging the time series (comparing Table 2 with Table 3). They are all significant. There were quite high positive correlations between AOD and CHL, CHL and SIC after shifting CHL 2 months (or more) ahead. However, the correlations between AOD and SIC, AOD and CLD showed no significant improvement after shifting AOD 1 month ahead.

We have found AOD was negatively correlated with CLD when lagged by one month (Tables 2 and 3). Here *P*-value are all less than 0.005.

The correlation coefficients between AOD and CLD were rather low. After shifting, the three most significant correlations were –0.65, –0.63, –0.93 for year 2003, 2009 and 2012 respectively. Year 2012 had very high negative correlation between CLD and AOD. The results show that AOD and CLD were less correlated compared to AOD and SIC.

3.6 *The relationship between DMS and SIC*

According to Simó's formula (Simó, 2002):

$$DMS = -\ln(MLD) + 5.7, \quad \text{when } CHL/MLD < 0.02; \tag{1a}$$

$$DMS = 55.8\,(CHL/MLD) + 0.6, \quad \text{when } CHL/MLD \geqslant 0.02. \tag{1b}$$

DMS is calculated using the satellite CHL and MLD mean time series within certain time frame and certain regions. There is ±30% uncertainty in the estimate DMS using above formula (Simó and Dachs, 2002). The double formula is not accurate for a different region in different time period influenced by different forcings. The double formula indicated the inverse relationship between DMS and MLD and positive relationship between DMS and CHL under certain conditions.

Due to the complicated MLD calculations from scattered field

Table 1. Correlation analysis for 75°–80°N for the ten years

Variables	Time lag	R^2	Std. error	*t*-statistic	*P*-value
AOD and SIC	1 month (SIC ahead)	0.39	0.000 23	6.56	0.001
AOD and CLD	1 month (CLD ahead)	0.18	0.055 67	–3.23	0.002
AOD and CHL	2 month (AOD ahead)	0.37	0.031 07	2.96	0.004
CHL and SIC	2–3 month (SIC ahead)	0.25	0.003 3	4.4	0.000 1

Note: SIC and CLD were both significantly correlated with AOD at a lag of one month, with AOD more strongly correlated with SIC. There were also significant moderate correlations between AOD and CHL for a lag of two months. The correlations between CHL and SIC were slightly different between 70°–75°N and 75°–80°N, with SIC 2 month ahead of CHL in 70°–75°N region (where CHL blooms earlier) and 3 month ahead of CHL in 75°–80°N.

Table 2. Correlations for the period of March to September

Year	AOD/SIC	AOD/CLD	AOD/CHL	CHL/SIC
2003	0.87	–0.47	–0.27	0.03
2004	0.70	0.25	–0.46	–0.21
2005	0.72	–0.57	0.04	–0.20
2006	0.84	–0.41	–0.31	–0.33
2007	0.78	–0.56	–0.37	0.11
2008	0.58	–0.29	–0.32	0.07
2009	–0.44	–0.01	0.02	–0.53
2010	0.97	–0.36	–0.01	–0.10
2011	0.68	–0.65	0.19	0.05
2012	0.76	–0.53	–0.72	–0.43

data, the time series of DMS were calculated using Eqs (1a, b) only for year 2003–2006. DMS flux then calculated together with profiles of SIC, CHL, AOD (shown in Fig. 12a). Peaks of CHL were 2 month behind SIC. The AOD had positive relationship with SIC for year 2003 and 2005 and negative relationship with SIC for year 2004 and 2006 during spring and early summer. AOD and SIC was decreased during summer period. There was slightly increase of AOD in September. DMS and CHL had similar peak time while DMS flux had its peak time 1–3 month ahead. The DMS flux peaks mostly occurred in spring rather than in summer. The reasons were due to the higher wind speed and more melting ice occurred in spring season in the region. There were increased trends from March to May and reduced trends from May to August for DMS concentration and AOD. Hence, during those two different periods, DMS and AOD were positively correlated. The melting ice accompanied by the increase of CHL and DMS. Generally, with increase of melting ice, DMS would increase accordingly. However, due to the rise of SST and solar radiation, the increasing rate of DMS would reduce or stop by May or June.

The ratio of DMS to SIC is calculated and plotted in Fig. 12b. The highest ratios for each year were different. May or June generally were the two peak months of the ratio, but year 2003 and 2004 had highest ratio towards September. The less SIC in September made the ratio higher. However, the SIC tended to be totally disappeared after year 2004. It is interesting to find that DMS/SIC ratio profile would exhibit the normal distributions after shifting SIC 2 months behind (Fig. 12c).

In Fig. 12a, DMS flux had positive correlations with SIC. They both had the same peak time for years 2005 and 2006, and year 2004 had much early SIC peak and the much later DMS flux peak (two months time lag). Peak of DMS flux was shifted ahead from June (2003) to March (2006). The peak of SIC was almost in March every year (year 2003 was slightly different). CHL and SIC had negative correlations before June and positive correlations after June.

SPSS software is used for correlation analysis for DMS and SIC. DMS and SIC had negative relationship with correlation coefficient of –0.575. The correlation is not significant.

The regression equation is as follows:

$$DMS = -0.981 + 2.003 \times SIC - 0.108 \times SIC^2 + 0.002 \times SIC^3,\ R^2 = 0.606. \quad (2)$$

In 70°–75°N and 75°–80°N two sub-region, DMS and SIC were negatively correlated with correlation coefficient around –0.5, the correlation is significant.

The three order model calculated the regression equation is

$$DMS = 10.434\text{–}0.881 \times SIC\text{–}0.028 \times SIC^2, \text{ for } 70^\circ\text{–}75^\circ\text{N}; \quad (3a)$$

$$DMS = \text{–}4.046 + 1.540 \times SIC\text{–}0.51 \times SIC^2, \text{ for } 75^\circ\text{–}80^\circ\text{N}. \quad (3b)$$

3.7 *Prediction of DMS flux in 4×CO_2*

The CMIP5 model archive is used to retrieve the forcing data for 4×CO_2 conditions. Software OpenLDAP is used to retrieve data for forcings such as SST, CLD, SIC, WIND and MLD. DMS model is used for calculating the regional DMS concentrations (Gabric et al., 1993, 1999; Qu and Gabric, 2010). A genetic algorithm is used for calibrating the key parameters in the DMS model (Qu and Gabric, 2010; Qu et al., 2016b). The satellite CHL mean time series is used for the calibration (to minimize the difference between the model output and the satellite data (CHL)). DMS observed data is also used to calibrate the parameters for DMS related parameters (Qu and Gabric, 2010; Qu et al., 2016b). The DMS model was run again using the newly calibrated parameters and the results of DMS flux for 70°–80°N are shown in Fig. 13 for 4×CO_2 with and without ice.

DMS flux is two times higher for 1×CO_2 (contemporary), and 1.5 times higher for 4×CO_2 when ice is considered. DMS flux increased more than 300% from 1×CO_2 to 4×CO_2. The increasing of melting ice could lead to an increase of CHL and the increase the DMS flux production.

The DMS flux rate under 4×CO_2 with ice considered increased much more than without ice considered. The SIC under 4×CO_2 condition was retrieved from CIMP5 (Coupled Model Intercomparison Project Phase 5). The increased autumn DMS flux is mainly due to the dramatic increase in sea-to-air transfer velocity. The more than 300% increase in DMS flux under 4×CO_2 sug-

Table 3. Lagged correlations for the period of March to September

	AOD and SIC (Shift AOD 1 month ahead)	AOD and CLD (Shift AOD 1 month ahead)	AOD and CHL (Shift CHL 2 month ahead)	CHL and SIC (Shift CHL 2 -3 month ahead)
2003	0.69	–0.65	0.71	0.63 (2 m)
2004	0.71	–0.20	0.88	0.93 (3 m)
2005	0.72	–0.84	0.71	0.99 (3 m)
2006	0.82	–0.46	0.64	0.995 (3 m)
2007	0.49	–0.37	0.52	0.56 (2 m)
2008	0.21	–0.48	0.79	0.74 (2 m)
2009	0.33	–0.63	0.37	0.85 (3 m)
2010	0.79	–0.60	0.83	0.92 (2 m)
2011	0.67	0.06	0.54	0.80 (2 m)
2012	0.67	–0.93	0.02	0.50 (2 m)

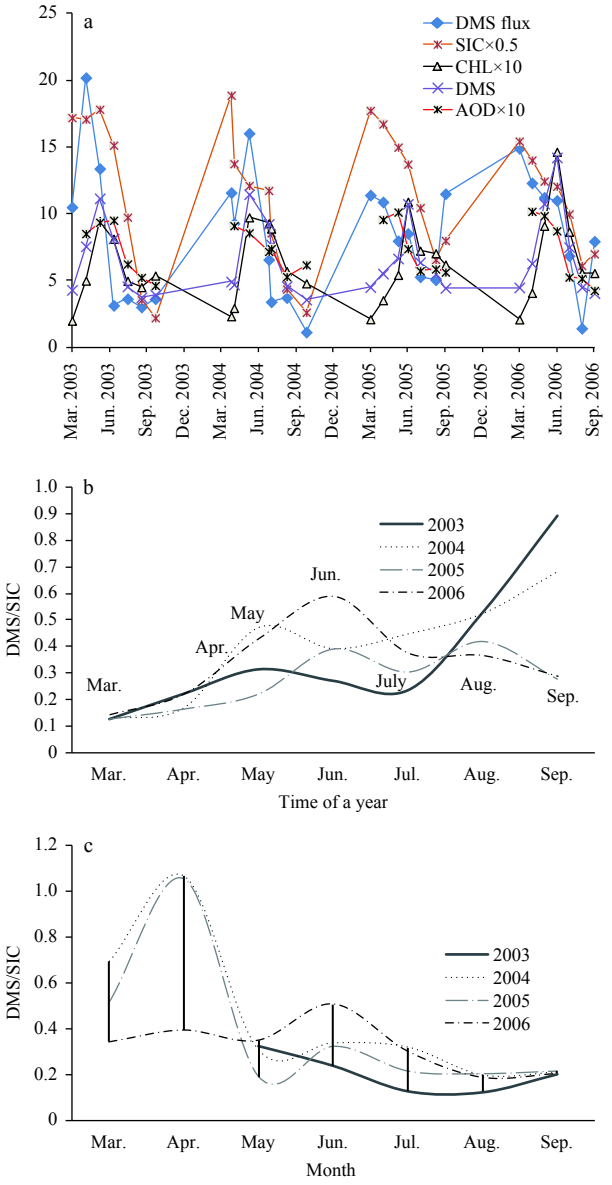

Fig. 12. Comparison among DMS flux (μmol/m^2), DMS (nmol/L), CHL (mg/m^3), SIC (%) and AOD in 70°–80°N (a); the DMS/SIC ratio plot for year 2003–2006 (b); and the DMS/SIC ratio plot after shifting SIC 2 month behind (c).

gests this would increase the indirect sulfate aerosol effect much more (Jones et al., 2001). The significant higher profile of DMS flux under ice condition suggested the melting ice is a major contributor to DMS flux from May to September. The more DMS flux released to atmosphere during summer and early autumn was the main reasons of elevated AOD in autumn.

4 Conclusions

The higher spring aerosols were mostly caused by Arctic haze and sea salt, while emission of autumn aerosols was likely due to biogenic sulfate aerosols (DMS) produced by the marine food web. Wind speed had an influence in the two different periods: spring and autumn. Sea salt aerosols increased with increasing of wind speed. Apart from the effect of Arctic haze caused by anthropogenic sources, sea salt aerosols also had an impact during the spring. It is difficult to distinguish the separate factors influ-

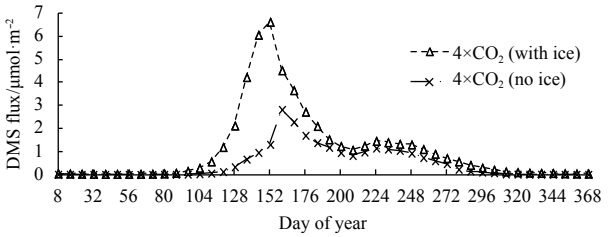

Fig. 13. Comparison of DMS flux with and without ice for 4×CO$_2$ in 70-80°N.

encing the seasonal aerosol cycle. The autumn increase in AOD indicated an increase in emissions of biogenic aerosols. DMS flux played a major role on the autumn elevated aerosols. The increased wind speed in autumn leading to an increased transfer velocity is the major reason of elevated autumn DMS flux. The ice melt in spring and summer also had significant impact DMS flux. This tendency would be magnified by year 2100 if the ice melt occurs earlier in the season.

The time series and correlation between AOD and SIC, AOD and melting ice, AOD and CLD (cloud cover) are examined. In contrast to CHL (which generally peaked in June), AOD was higher in spring and lower in summer. Usually there was a little increase of AOD in autumn due to the emission of biogenic aerosols possibly associated with phytoplankton synthesis of DMS. Interannual variability of AOD was high. Year 2009 had higher AOD and year 2010 had lower AOD. In most years, SIC was positively correlated with AOD in spring and early summer and negatively correlated in late summer and autumn. DMS concentration was calculated by using Simó's formula. The calculations could cause some errors. However, the profiles are the indications. More accurate DMS calculation using different approach is expected to carry out in the future.

Our results for year 2003–2006 show that DMS and CHL had similar peak time and positively correlated. DMS flux had peak in spring due to the high wind speed. DMS concentration, CHL and AOD presented increased trends before May and decreased trends from May to August. Both SIC and CLD were all around one month ahead of AOD and there were good correlations between AOD and SIC and poor correlations between AOD and CLD. Wind speed was generally over 7 m/s and elevated high wind speed from autumn to next spring (not shown) had an effect on AOD concentrations. SIC, surface wind speed and SST were the main physical drivers of sea salt aerosol (Nilsson et al., 2007), while SIC played a significant role in the Arctic (Qu et al., 2016b).

However, DMS may not play a critical role in regulating the cloud formation (Quinn and Bates, 2011). Some other gases may also impact it (such as isoprene (Meskhidze and Nenes, 2010) and sea salt, etc.). Thus, the DMS flux may possibly offset the climate warming but not affirmative. However, in the Greenland Sea, DMS flux is more related to the ice melting and it may have significant impact to the regional climate as we predicted. When SIC dramatic decreasing, more ice free water of Arctic Ocean would make the oceanic input of gaseous aerosol precursors into the atmosphere become more important.

Future changes in anthropogenic aerosol sources cannot be ignored but the impact on the local and global aerosols is difficult to access. Unravelling the relation between CLD and AOD is difficult, as one signal can contaminate the other in satellite data. If greenhouse-gas emissions decrease, the predicted increase of

biogenic sulfate aerosol in the Arctic Ocean may help reduce future warming (Levasseur, 2013; Qu et al., 2016b). However, if emissions of the short life-time sulfate aerosol do not keep pace with the long-lived greenhouse-gases, polar warming will continue to accelerate.

Acknowledgements

The authors are grateful to NASA's Ocean Biology Processing Group for providing MODIS aqua, Level 3 (4-km equi-rectangular projection) 8-day mapped global data for chlorophyll *a* (CHL) and aerosol optical depth (AOD). We thank the NASA Web SeaDAS development group for providing ocean colour SeaDAS Software (SeaWiFS Data Analysis System) for processing regional CHL and AOD data. Thanks to NOAA NCEP EMC CMB GLOBAL Reyn-SmithOIv2 for providing weekly and monthly sea-ice concentration. Thanks to the NASA Earth Science MEaSUREs DISCOVER Project and the NASA Earth Science Physical Oceanography Program for providing Wind Data and Sea Surface Temperature data and NASA for providing cloud cover data (http://gdata1.sci.gsfc.nasa.gov). Thanks to Ren Hongjian from School of Computer Science and Technology in Nantong University for helping with the wind data.

References

Andreae M O. 2007. Aerosols before pollution. Science, 315(5808): 50–51

Bailey S W, Werdell P J. 2006. A multi-sensor approach for the on-orbit validation of ocean color satellite data products. Remote Sensing of Environment, 102(1–2): 12–23

Barrie L A. 1995. Arctic aerosols: Composition, sources and transport. In: Delmas R J, ed. Ice Core Studies of Global Biogeochemical Cycles. Berlin, Heidelberg: Springer, 1–22

Charlson R J, Lovelock J E, Andreae M O, et al. 1987. Oceanic phytoplankton, atmospheric sulphur, cloud albedo and climate. Nature, 326(6114): 655–661

Chaves J E, Werdell P J, Proctor C W, et al. 2015. Assessment of ocean color data records from MODIS-Aqua in the western Arctic Ocean. Deep Sea Research Part II: Topical Studies in Oceanography, 118: 32–43

Curry J A. 1995. Interactions among aerosols, clouds, and climate of the Arctic Ocean. Science of the Total Environment, 160–161: 777–791

Curry J A, Rossow W B, Randall D, et al. 1996. Overview of arctic cloud and radiation characteristics. Journal of Climate, 9(8): 1731–1764

Ferek R J, Hobbs P V, Radke L F, et al. 1995. Dimethyl sulfide in the Arctic atmosphere. Journal of Geophysical Research: Atmospheres, 100(D12): 26093–26104

Fitch D T, Moore J K. 2007. Wind speed influence on phytoplankton bloom dynamics in the Southern Ocean Marginal Ice Zone. Journal of Geophysical Research: Oceans, 112(C8): C08006

Gabric A J, Cropp R, Hirst T, et al. 2003. The sensitivity of dimethyl sulfide production to simulated climate change in the Eastern Antarctic Southern Ocean. Tellus B, 55(5): 966–981

Gabric A J, Matrai P A, Vernet M. 1999. Modelling the production and cycling of dimethylsulphide during the vernal bloom in the Barents Sea. Tellus B, 51(5): 919–937

Gabric A, Murray N, Stone L, et al. 1993. Modelling the production of dimethylsulfide during a phytoplankton bloom. Journal of Geophysical Research: Ocean, 98(C12): 22805–22816

Gabric A J, Qu B, Matrai P A, et al. 2005. The simulated response of dimethylsulfide production in the Arctic Ocean to global warming. Tellus B, 57(5): 391–403

Gabric A J, Qu B, Rotstayn L, et al. 2013. Global simulations of the impact on contemporary climate of a perturbation to the sea-to-air flux of dimethylsulphide. Australian Meteorology and Oceanographic Journal, 63(3): 365–376

Gabric A J, Simó R, Cropp R A, et al. 2004. Modeling estimates of the global emission of dimethylsulfide under enhanced greenhouse conditions. Global Biogeochemical Cycles, 18(3): GB3016

Hu Ting, Sun Zhaobo, Li Zhaoxin. 2011. Features of aerosol optical depth and its relation to extreme temperatures in China during 1980–2001. Acta Oceanologica Sinica, 30(2): 33–45

Huang Chuanjiang, Qiao Fangli. 2009. The relationship between sea surface temperature anomaly and wind energy input in the Pacific Ocean. Progress in Natural Science, 19(10): 1409–1412

Leck C, Persson C. 1996. Seasonal and short-term variability in dimethyl sulfide, sulfur dioxide and biogenic sulfur and sea salt aerosol particles in the arctic marine boundary layer during summer and autumn. Tellus B, 48(2): 272–299

Levasseur M. 2013. Impact of Arctic meltdown on the microbial cycling of sulphur. Nature Geoscience, 6(9): 691–700

Jones A, Roberts D L, Woodage M J, et al. 2001. Indirect sulphate aerosol forcing in a climate model with an interactive sulphur cycle. Journal of Geophysical Research: Atmospheres, 106(D17): 20293–20310

Meskhidze N, Nenes A. 2010. Effects of ocean ecosystem on marine aerosol-cloud interactions. Advances in Meteorology, 2010: 239808

Nilsson E D, Mårtensson E M, Van Ekeren J S, et al. 2007. Primary marine aerosol emissions: size resolved eddy covariance measurements with estimates of the sea salt and organic carbon fractions. Atmospheric Chemistry and Physics Discussions, 7(5): 13345–13400

Osto M D, Beddows D C S, Tunved P, et al. 2017. Arctic sea ice melt leads to atmospheric new particle formation. Scientific Reports, 7: doi: 10.1038/s41598-017-03328-1

Pang Hao. 2006. Econometrics (in Chinese). Beijing: Science Press

Qu Bo, Gabric A J. 2010. Using genetic algorithms to calibrate a dimethylsulfide production model in the Arctic Ocean. Chinese Journal of Oceanology and Limnology, 28(3): 573–582

Qu Bo, Gabric A J, Lu Hailang, et al. 2014. Spike in phytoplankton biomass in Greenland Sea during 2009 and the correlations among chlorophyll-a, aerosol optical depth and ice cover. Chinese Journal of Oceanology and Limnology, 32(2): 241–254

Qu Bo, Gabric A J, Lu Zhiferng, et al. 2016a. Unusual phytoplankton bloom phenology in the northern Greenland Sea during 2010. Journal of Marine Systems, 164: 144–150, doi: 10.1016/j.jmarsys.2016.07.011

Qu Bo, Gabric A J, Zeng Meifang, et al. 2016b. Dimethylsulfide model calibration in the Barents Sea using a genetic algorithm and neural network. Environmental Chemistry, 13(2): 413–424

Quinn P K, Bates T. 2011. The case against climate regulation via oceanic phytoplankton sulphur emissions. Nature, 480(7375): 5–16

Quinn P K, Shaw G, Andrews E, et al. 2007. Arctic haze: current trends and knowledge gaps. Tellus B, 59(1): 99–114

Reynolds R W, Rayner N A, Smith T M, et al. 2002. An improved in situ and satellite SST analysis for climate. Journal of Climate, 15(13): 1609–1625

Serreze M C, Walsh J E, Chapin III F S, et al. 2000. Observational evidence of recent change in the northern high-latitude environment. Climatic Change, 46(1–2): 159–207

Simó R, Dachs J. 2002. Global ocean emission of dimethylsulfide predicted from biogeophysical data. Global Biogeochemical Cycles, 16(4): 1078

Spracklen D V, Bonn B, Carslaw K S. 2008. Boreal forests, aerosols and the impacts on clouds and climate. Philosophical Transactions of the Royal Society A: Mathematical, Physical and Engineering Sciences, 366(1885): 4613–4626

Struthers H, Ekman A M L, Glantz P, et al. 2011. The effect of sea ice loss on sea salt aerosol concentrations and the radiative balance in the Arctic. Atmospheric Chemistry and Physics, 11(7): 3459–3477

Zhao Chuanfeng, Garrett T J. 2014. Effects of Arctic haze on surface cloud radiative forcing. Geophysical Research Letters, 42(2): 557–564